

Synthesis of Ferrocenyl-Based Unsymmetrical Azines via a Simple Reaction of Aldehydes with Ketone-Derived *N*-Tosyl Hydrazones and the Evaluation of the Extent of Conjugation in the Molecule

Junyang Dong,[†] Yufeng Liu,[†] Jianfeng Hu,^{†,‡} Qiang Teng,[†] Jianhua Cheng,[§] Yi Luo,^{||}
and Hao Zhang^{*,†,‡,§,||}

[†]School of Chemical & Chemical Engineering, Inner Mongolia University, Hohhot 010021, People's Republic of China

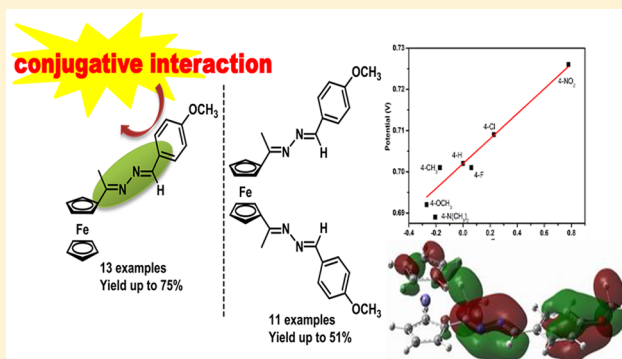
[‡]Inner Mongolia Key Laboratory of Fine Organic Synthesis, Hohhot 010021, People's Republic of China

[§]State Key Laboratory of Polymer Physics and Chemistry, Changchun Institute of Applied Chemistry, Chinese Academy of Sciences, Changchun 130022, People's Republic of China

^{||}State Key Laboratory of Fine Chemicals, School of Chemical Engineering, Dalian University of Technology, Dalian 116024, People's Republic of China

S Supporting Information

ABSTRACT: We have designed and synthesized 1-substituted and 1,1'-disubstituted ferrocene-based unsymmetrical azines under metal-free conditions. The crystal structures of **3k**, **5i**, and **5g** revealed that conjugative interactions between the ferrocene phenyl rings and the entire azine fragment exist. Furthermore, our electrochemical and optical analysis provided support for extended conjugation, which suggested a larger substituent effect in this system. Density functional theory calculations also supported the results. Thus, these results reflect a stronger conjugative interaction between the ferrocene phenyl rings and the entire azine fragment.



■ INTRODUCTION

Azines are one of a number of very important compounds that have interesting chemical properties. Among their useful properties, azines have attracted great interest due to their potential in biological properties,¹ in the design of liquid crystals,^{2–4} and in other materials applications.^{5–7} Molina's and our group reported the application of azines as a recognition unit in chemosensors,^{8,9} which had high selectivity toward Hg^{2+} or Cu^{2+} ions. Moreover, our group demonstrated that 1-substituted ferrocene-based unsymmetrical azines that have different substituent groups on the phenyl have significant influence on the sensitivity. For example, ferrocene-based unsymmetrical azines which contain a strongly electron withdrawing group (4-NO_2) did not exhibit any recognition toward Cu^{2+} or Hg^{2+} ions. With the binding of azines and Hg^{2+} or Cu^{2+} ions, the fluorescence signal changed obviously, which may be explained by the quenching of the fluorescence of pyrene unit in the neutral chemosensor by the ferrocene unit. In the quenching process, the azine units act as an electron or energy transfer bridge from the ferrocene unit to pyrene unit. Though the symmetrical and asymmetrical aryl-substituted acetophenone azines may be "conjugation stoppers",^{10,11} the conjugation in ferrocenyl-based unsymmetrical azines is still unclear. To the best of our knowledge, it is due to the lack of an

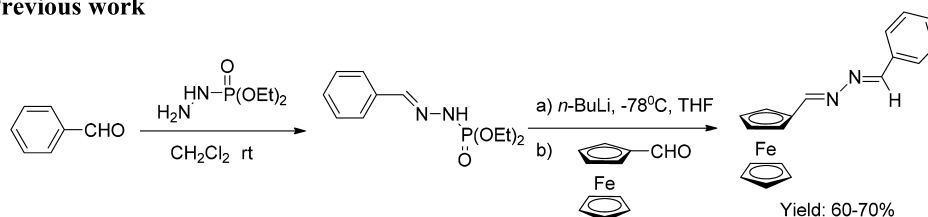
appropriate synthetic method to prepare various types of azines. Only a few examples of ferrocene-based unsymmetrical azines have been reported by using Zwierzak's method recently,¹² which required *n*-butyllithium at a very low temperature ($-78\text{ }^{\circ}\text{C}$).

In view of the importance of ferrocenyl-based unsymmetrical azines and the limitations of established methods, it is desirable to develop highly efficient synthetic strategies for the rapid construction of ferrocenyl-based unsymmetrical azines (Scheme 1). Recently, *N*-tosyl hydrazones have emerged as a new type of cross-coupling partner in C–C bond formation, including their reactions with aryl halides,¹³ arylsulfonates,¹⁴ alkynes,^{15–17} azoles,^{18,19} arylboronic acids,^{20,21} benzylic halides,²² etc. More recently, Wei and co-workers have demonstrated that the azines could be prepared by the reaction of tosyl hydrazones, aldehydes, and PPh₃.^{23,24} We developed an easy and efficient method to synthesize various 1-substituted ferrocene-based unsymmetrical azines.⁹ More remarkably, 1,1'-disubstituted ferrocene-based unsymmetrical azines were also obtained through this method.⁹ In addition, the evaluation of the extent of conjugation in ferrocene-based unsymmetrical azines was

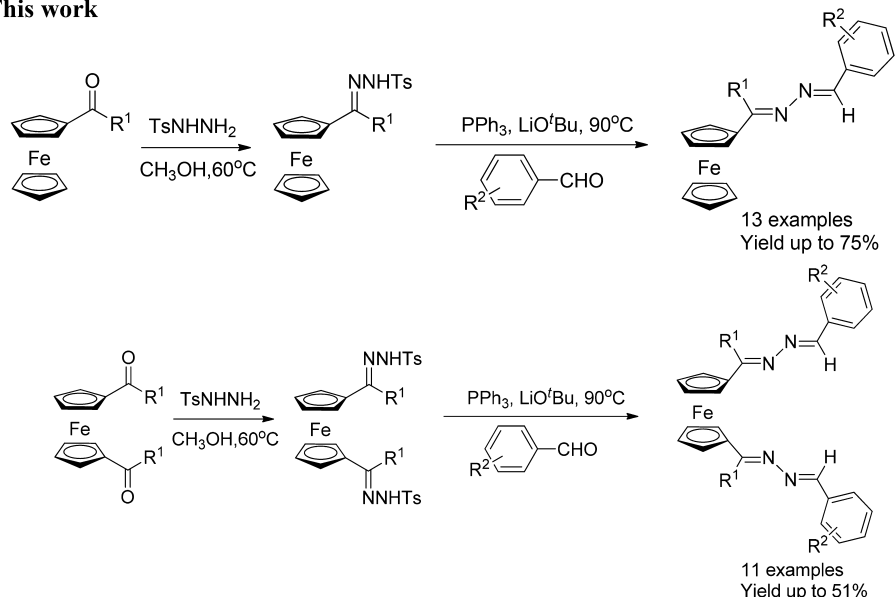
Received: May 12, 2017

Scheme 1. Methods for Preparing the Ferrocenyl-Based Unsymmetrical Azines

Previous work



This work



also studied by using the solid state (X-ray and DFT calculations) and methods (UV–vis and electrochemical).

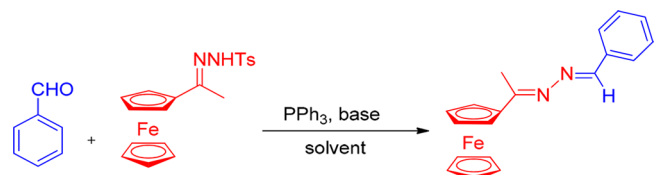
RESULTS AND DISCUSSION

For the preliminary study, the reaction of aryl aldehyde **1a**, ferrocenyl methyl ketone derived *N*-tosyl hydrazone²⁵ **2a**, and PPh_3 was examined (Table 1). Initially **1a** (1 equiv) and **2a** (1.2 equiv) were treated with PPh_3 (1.2 equiv) and LiOtBu (1.2 equiv) in dioxane at 90°C for 16 h. To our delight, the expected product **3a** was obtained in 42% yield under the initial conditions (Table 1, entry 1). Furthermore, it was found that the expected product **3a** could be obtained in 52% yield by using 2 equiv of aryl aldehyde **1a** (Table 1, entry 2). To optimize the reaction conditions, we carefully examined the effect of the bases on this reaction. LiOtBu was found to be the most suitable base for this transformation (Table 1, entry 7). Other bases, such as NaOtBu , KOtBu , K_2CO_3 , and Cs_2CO_3 , also worked for this reaction, though in lower yields (Table 1, entries 8–11). Screening of solvents indicated that toluene was optimal, while the other solvents, DCE, THF, CH_3CN , and DMF afforded the desired product in much lower yields (Table 1, entries 12–16). The temperature and reaction time were found to influence the reactivity (Table 1, entries 17–20). For example, the yield decreased to 58% when the temperature was lowered to 80°C . Finally, the optimized conditions were obtained: aryl aldehyde **1a** (0.5 mmol), ferrocenyl methyl ketone derived *N*-tosyl hydrazone **2a** (0.25 mmol), PPh_3 (0.5 mmol), and LiOtBu (0.275 mmol) in dioxane at 90°C (Table 1, entry 10).

With the optimized conditions, we next investigated the scope of the reaction (Table 2). The reaction system displayed good tolerance toward a range of functional groups. Ferrocenyl alkyl ketone groups (products **3a–c**) were all tolerated. However, when ferrocenyl aromatic ketone groups were used, no desired product was obtained. A variety of electron-rich, electron-neutral, and electron-deficient aryl aldehydes underwent the reaction smoothly to afford the desired products in good yields (products **3d–k**). Notably, products substituted with 2-thienyl (**3l**) and 9-anthryl groups (**3m**)^{9,26} could also be obtained in good yields. It should be mentioned that high stereoselectivities were observed in all compounds and only the *E,E* conformation was obtained, as observed in solution by ^1H NMR spectroscopy.

Furthermore, we proceeded to apply this system to 1,1'-ferrocenyl diketone derived *N*-tosyl hydrazone²⁵ **4a** with a similar aryl aldehyde **1a**. To our delight, it was found that the expected product **5a**²⁷ could be obtained in 51% yield with a slightly increased loading of PPh_3 and base. The reaction system displayed good tolerance toward a range of functional groups. A series of 1,1'-ferrocenyl diketone derived *N*-tosyl hydrazones bearing substituents such as methyl, ethyl, and *n*-propyl all worked well in the reaction, affording the expected products in moderate yields (Table 3, **5a–c**). A variety of aryl aldehydes can also be easily obtained (Table 3, **5d–i**). It is worth noting that 2-thienyl- and 9-anthryl-substituted aldehydes (**1j,k**) could be transformed suitably to **5j,k**, respectively.

Solid-State Study of Ferrocenyl-Based Unsymmetrical Azines. The structures of **3d** (4-Cl), **3e** (4-F), **3f** (4-Me), **3k** (4-OMe), **5g** (4- $\text{N}(\text{Me})_2$), and **5i** (4-OMe) were confirmed by X-ray crystallography (Figure 1). Table 4 gives some selected

Table 1. Optimization of Reaction Conditions^a


entry	2a:1a	PPh ₃ (equiv)	solvent (mL)	base (equiv)	<i>t</i> (°C)	time (h)	yield ^b (%)
1	1:1.2	1.2	dioxane (5)	LiO ^t Bu (1.2)	90	16	42
2	1:2.0	1.2	dioxane (5)	LiO ^t Bu (1.2)	90	16	52
3	1:1.2	2.0	dioxane (5)	LiO ^t Bu (1.2)	90	16	62
4	1:1.2	3.0	dioxane (5)	LiO ^t Bu (1.2)	90	16	64
5	1:1.2	1.2	dioxane (5)	LiO ^t Bu (1.1)	90	16	51
6	1:1.2	1.2	dioxane (5)	LiO ^t Bu (2.0)	90	16	19
7	1:2.0	2.0	dioxane (5)	LiO ^t Bu (1.1)	90	16	75
8	1:2.0	2.0	dioxane (5)	KO ^t Bu (1.1)	90	16	21
9	1:2.0	2.0	dioxane (5)	K ₂ CO ₃ (1.1)	90	16	12
10	1:2.0	2.0	dioxane (5)	Cs ₂ CO ₃ (1.1)	90	16	38
11	1:2.0	2.0	dioxane (5)	NaO ^t Bu (1.1)	90	16	70
12	1:2.0	2.0	toluene (5)	LiO ^t Bu (1.1)	90	16	71
13	1:2.0	2.0	DCE (5)	LiO ^t Bu (1.1)	90	16	48
14	1:2.0	2.0	THF (5)	LiO ^t Bu (1.1)	90	16	65
15	1:2.0	2.0	CH ₃ CN (5)	LiO ^t Bu (1.1)	90	16	63
16	1:2.0	2.0	DMF (5)	LiO ^t Bu (1.1)	90	16	67
17	1:2.0	2.0	dioxane (5)	LiO ^t Bu (1.1)	80	16	58
18	1:2.0	2.0	dioxane (5)	LiO ^t Bu (1.1)	110	16	65
19	1:2.0	2.0	dioxane (5)	LiO ^t Bu (1.1)	90	12	63
20	1:2.0	2.0	dioxane (5)	LiO ^t Bu (1.1)	90	24	76

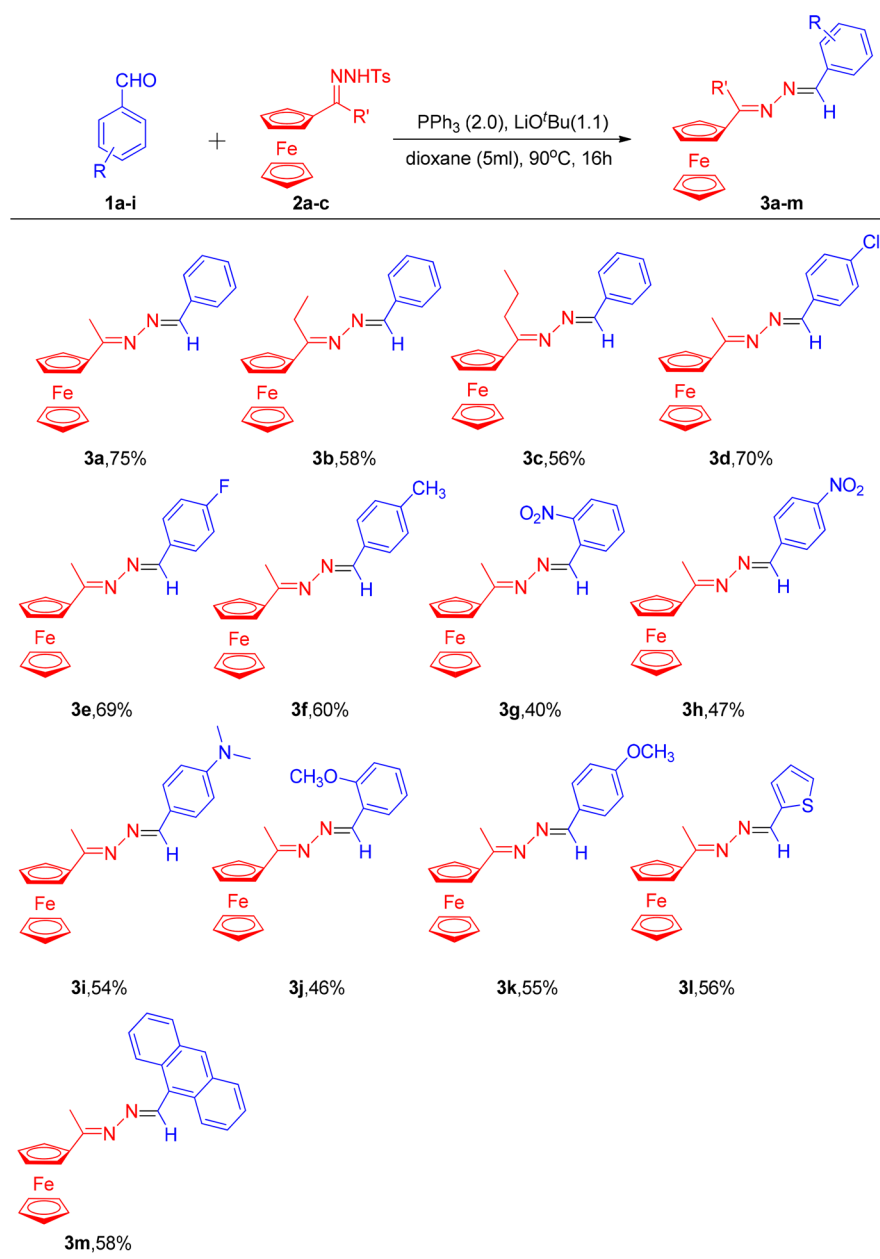
^aReactions were carried out with benzaldehyde **1a** (0.5 mmol), ferrocenyl methyl ketone derived *N*-tosyl hydrazone **2a** (0.25 mmol), and PPh₃ (0.5 mmol) in the presence of 1.1 equiv of base under a N₂ atmosphere. ^bYield of the isolated product after chromatography.

bond lengths (Å), angles (deg), and torsion angles (deg) for **3k** (4-OMe), **3f** (4-Me), **3d** (4-Cl), **3e** (4-F), **5g** (4-N(Me)₂), and **5i** (4-OMe). The gauche conformations with torsion angles, -C=N-N=C-, of -162.1° for **3d** (4-Cl), -177.40° for **3e** (4-F), -177.70° for **3f** (4-Me), 174.3° for **3k** (4-OMe), 172.2 and 163.6° for **5g** (4-N(Me)₂), and 179.0 and 160.1° for **5i** (4-OMe), which indicated the structure of -C=N-N=C-, were a more nearly planar conformations in comparison to the reported azines.^{10,11} The torsion angle (-C=N-N=C-) of phenyl/4-OCH₃¹¹ was 136.0°, which was significantly smaller than that of the corresponding **3k** (4-OMe). The C-C bonds of the Cp ring generally deviate in the ranges of 1.394–1.407 and 1.377–1.420 Å for **3k** (4-OMe), 1.401–1.429 and 1.392–1.425 Å for **5g** (4-N(Me)₂), and 1.403–1.440 and 1.406–1.427 Å for **5i** (4-OMe). The lengths of the C-C bonds involving the C atom attached to the substituent differ significantly. The C-C bonds of benzene ring deviate in the range of 1.368–1.404 Å for **3k** (4-OMe), 1.368–1.399 and 1.359–1.395 Å for **5g** (4-N(Me)₂), and 1.376–1.389 and 1.364–1.396 Å for **5i** (4-OMe). The lengths of the C-C bonds involving the C atom attached to the substituent also differ significantly. Generally, the C=N bond lengths of **3k** (4-OMe), **5g** (4-N(Me)₂), and **5i** (4-OMe) are in the range of 1.258–1.285 Å, which are close to the 1.279 Å for C_{sp2}=N bond lengths and close to the C=N bond length of 1.276 Å in formaldoxime.³⁰ The C=N bond lengths 1.273 and 1.266 Å of **3k** (4-OMe) are shorter than corresponding phenyl/4-OCH₃ lengths of 1.280 and 1.277 Å,¹¹ which may be due to the fact that ferrocenyl is a more electron donating group than phenyl and causes the electron cloud

density of **3k** (C=N) to be enhanced. The C-C bonds between the azine C and ferrocenyl C atoms are in the range of 1.460–1.470 Å, which are slightly shorter than 1.485 Å for a normal C_{sp2}-C_{sp2} single bond. However, the C-C bonds between the azine C and aromatic C atoms are in the range of 1.443–1.459 Å, which are much shorter than a normal C_{sp2}-C_{sp2} single bond. The N-N bond lengths of **3d** (4-Cl), **3e** (4-F), **3f** (4-Me), **3k** (4-OMe), **5g** (4-N(Me)₂), and **5i** (4-OMe) are in the range of 1.401–1.413 Å. They are shorter than 1.47 Å, which is the generally accepted N-N single bond length, and these shortenings are expected for N-N bonds between sp²-hybridized N atoms. The N-N bond length (1.408 Å) of phenyl/4-OCH₃¹¹ is longer than that of the ferrocenyl derivative **3k** (4-OMe) (1.401 Å). It is concluded that shorter C-C and N-N bond lengths are indicative of double-bond character resulting from contributions of resonance forms reflecting extensive conjugation over the entire molecule. The dihedral angle of phenyl/4-OCH₃¹¹ (30.2°) was much larger than that of **3k** (4-OCH₃) (7.2°). The most striking feature of the angle between the aryl ring and the central -C=N-N=C- moiety, only 3.7°, may indicate the almost complete planarity of the **3f** (4-CH₃) fragment (Table 5). When the above results are taken into account, it might be suggested that conjugative interactions between the ferrocene phenyl rings with the entire azine fragment exist in these ferrocenyl compounds.

Liquid State Study of Ferrocenyl-Based Unsymmetrical Azines. The electrochemical behavior of the series of monosubstituted ferrocenyl-based unsymmetrical azines **3a** (4-

Table 2. Preparation of Ferrocenyl-Based Unsymmetrical Azines **3** from the Reaction of Ferrocenyl Ketone Derived *N*-Tosyl Hydrazones, Aldehydes, and PPh_3 ^a



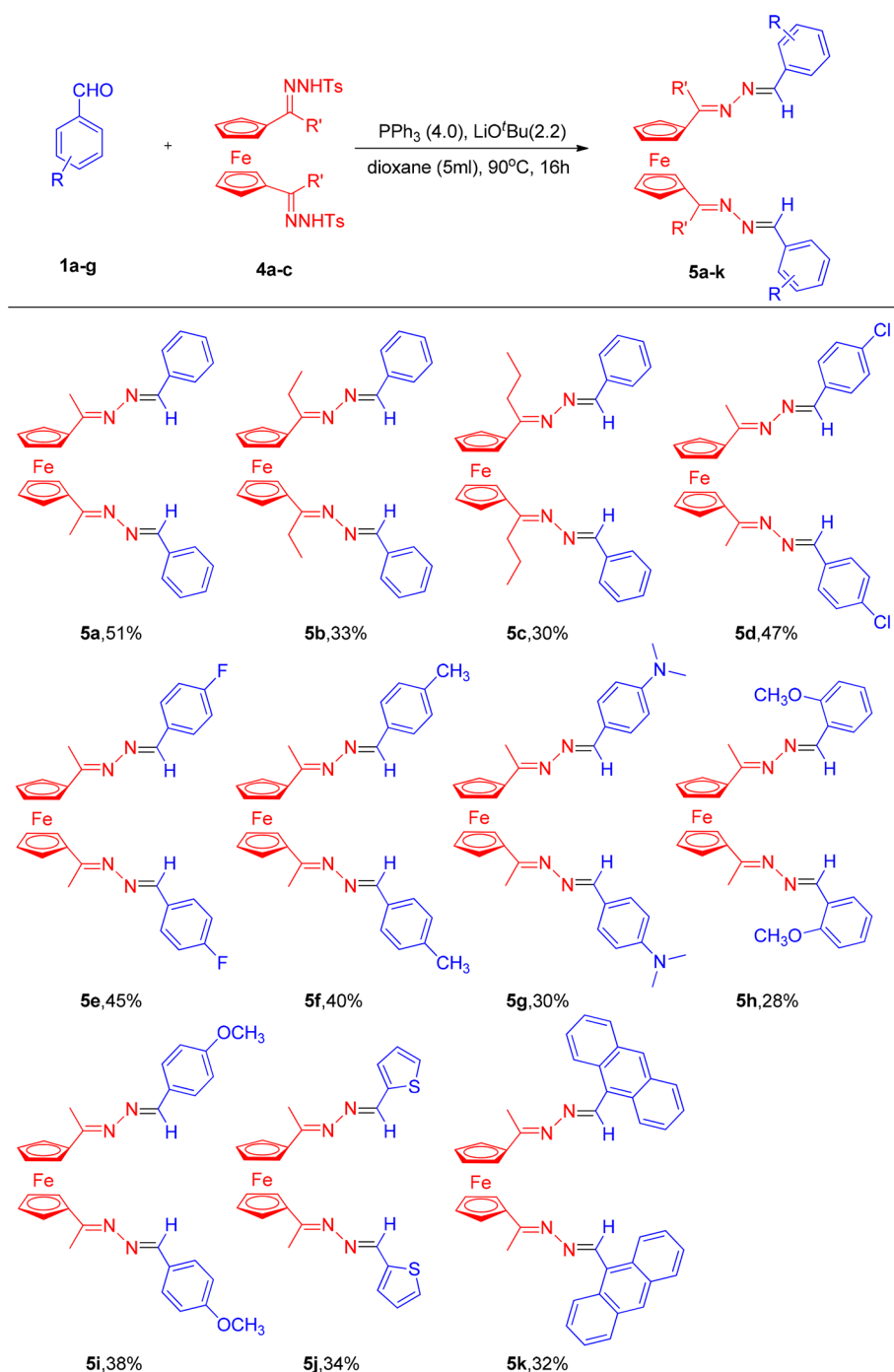
^aReaction conditions: aryl aldehydes **1a–i** (0.5 mmol), ferrocenyl ketone derived *N*-tosyl hydrazones **2a–c** (0.25 mmol), PPh_3 (0.5 mmol), LiOtBu (0.275 mmol), dioxane (5 mL), 90 °C, 16 h. Isolated yields are given. The compounds **3a**,⁹ **3c**,⁹ **3h**,^{9,28} **3j**,⁹ **3k**,⁹ and **3m**^{9,26} have been reported.

H), **3d** (4-Cl), **3e** (4-F), **3f** (4-CH₃), **3h**^{9,28} (4-NO₂), **3i** (4-N(CH₃)₂), and **3k** (4-OCH₃) was studied in acetonitrile (CH₃CN) solution using cyclic voltammetry.

As shown in Figure 2, cyclic voltammetry displayed a reversible oxidation at 0.1 V s⁻¹ due to the ferrocene/ferrocenium redox couple.⁹ This result illustrated a significant substituent effect on the single-electron oxidation. The more electrons that are withdrawn, the easier the substituent azine is to oxidate and the more positive is the E° value. The oxidation potentials of the aryl azines can be correlated with Hammett σ parameters to examine variations in E° as a function of substituent. As shown in Figure 3, the plot shows distinct correlations for the oxidation potentials of the ferrocenyl-based azines of the substituents. F is a more electron withdrawing

group than Cl, but the $-\text{C}=\text{N}-\text{N}=\text{C}-$ unit of **3e** (4-F) was not completely conjugated (Figure 7). This is the reason that **3e** (4-F) did not have a more positive E° . The electrochemical behavior of 1,1'-disubstituted ferrocenyl-based unsymmetrical azines **5a**²⁷ (4-H), **5d** (4-Cl), **5e** (4-F), **5f** (4-CH₃), **5g** (4-N(CH₃)₂), and **5i** (4-OCH₃) was studied under the same conditions (Figure 4). The results are similar to those for the monosubstituted ferrocenyl-based unsymmetrical azines. Importantly, in comparison with 1,1'-disubstituted ferrocenyl-based unsymmetrical azines ($E^\circ_{4\text{-OCH}_3} = 0.576$ V), the monosubstituted ferrocenyl-based unsymmetrical azines ($E^\circ_{4\text{-OCH}_3} = 0.692$ V) are easier to oxidize. In these cases, these results suggested a more substantial substituent effect on

Table 3. Preparation of Ferrocenyl-Based Unsymmetric Azines **5** from the Reaction of 1,1'-Ferrocenyl Diketone Derived *N*-Tosyl Hydrazone, Aldehydes, and PPh_3 ^a



^aReaction conditions: aryl aldehydes **1a–g** (0.5 mmol), ferrocenyl ketone derived *N*-tosyl hydrazones **4a–c** (0.25 mmol), PPh_3 (1 mmol), LiO^tBu (0.55 mmol), dioxane (5 mL), 90 °C, 16 h. Isolated yields. The compounds **5a**,²⁷ **5i**,²⁹ and **5k**⁹ have been reported.

the electrochemical properties. These results further provided support for extended conjugation in this system.

To further examine the characteristics of the ferrocenyl-based unsymmetrical azines, the UV–vis spectra were measured. Representative UV–vis spectra of the monosubstituted ferrocenyl-based unsymmetrical azines are shown in Figure 5, and the λ_{max} values are summarized in Table 6. The more electron-donating the substituent, the easier the ferrocenyl-based azine is to red shift. In contrast with the electron-donating substituents, the UV–vis spectra of the monosub-

stituted ferrocenyl-based azines with electron-withdrawing substituents changed less (Table 6). However, the ferrocenyl-based unsymmetrical azine **3h**^{9,28} (4- NO_2) experienced an obvious red shift. The UV–vis spectra of 1,1'-disubstituted ferrocenyl-based unsymmetrical azines **5a**²⁷ (4-H), **5d** (4-Cl), **5e** (4-F), **5f** (4- CH_3), **5g** (4- $\text{N}(\text{CH}_3)_2$), and **5i** (4- OCH_3) were investigated (Figure 6). In comparison with monosubstituted ferrocenyl-based unsymmetrical azines, an absorption at 426 nm produced by the ligand to metal charge transfer (LMCT) transition of 1,1'-disubstituted ferrocenyl-based unsymmetrical

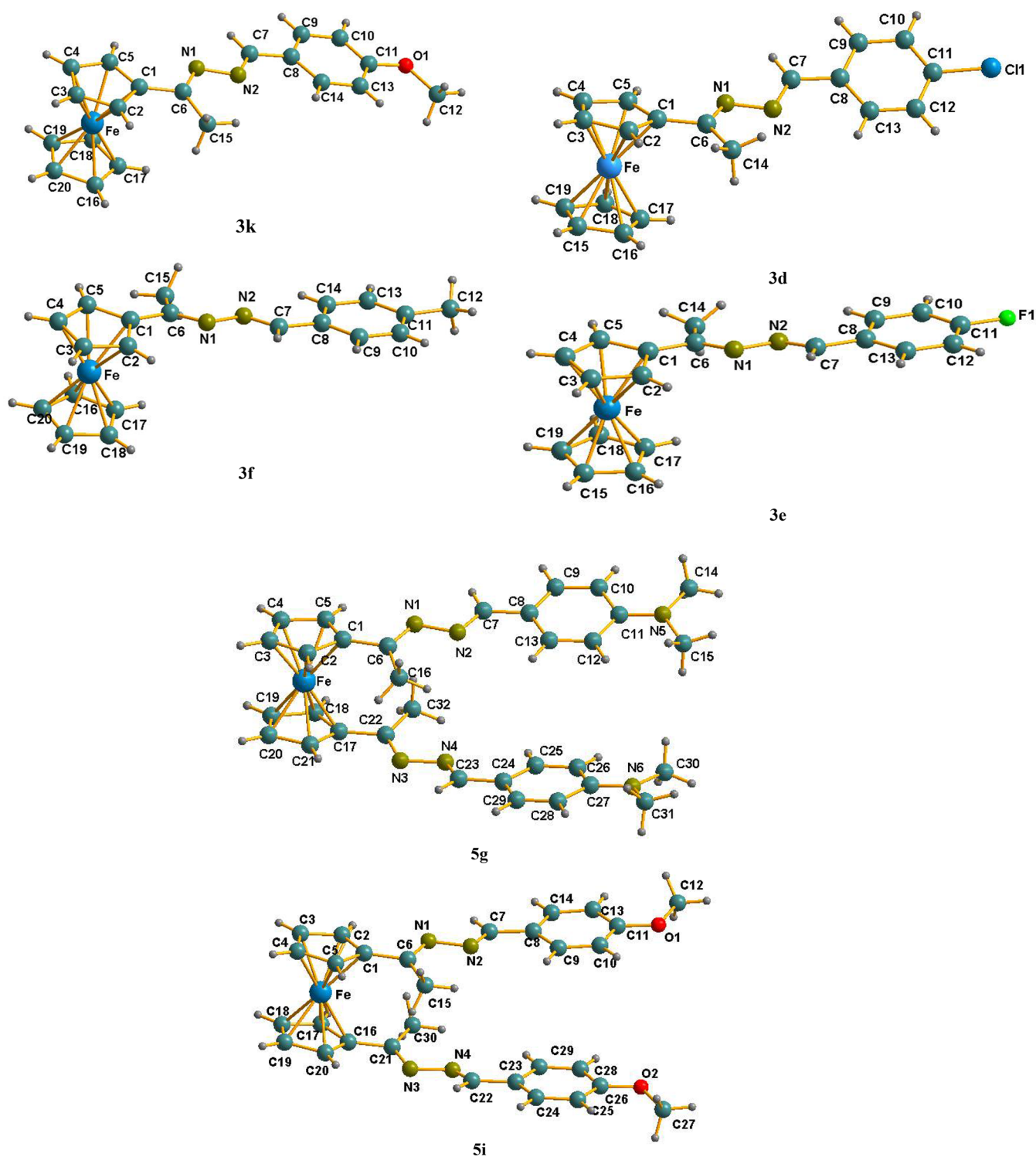


Figure 1. X-ray structures of the compounds **3k**, **3f**, **3d**, **3e**, **5g**, and **5i**.

azines arose. The great change may be due to a stronger conjugative interaction. These results were coupled with the larger substituent effect on the ferrocenyl-based unsymmetrical azines. Our electrochemical and optical analysis provided support for extended conjugation in this system.

Calculations were also performed to qualitatively examine the structures of azines. As a guide, these calculations were performed for an analysis of the electrochemical and optical studies. As shown in Figure 7, the HOMO of the phenyl/4-

OCH₃¹¹ is mainly localized on the CH₃O-aryl fragment. Meanwhile, the HOMO of the ferrocenyl/4-F and ferrocenyl/4-CH₃ is also mainly localized on F-aryl or CH₃-aryl. Furthermore, the qualitative indication indicated that the HOMO of the phenyl azine (phenyl/4-OCH₃) and ferrocenyl azines (ferrocenyl/4-F and ferrocenyl/4-CH₃) made a less significant contribution on the azine –C=N–N=C– unit, as determined by the calculations. Importantly, the qualitative indication indicated that the the HOMO of the ferrocenyl azine

Table 4. Selected Bond Lengths (Å), Angles (deg), and Torsion Angles (deg) for 3k, 3f, 3d, 3e, 5g, and 5i

	3k (4-OMe)	3f (4-Me)	3d (4-Cl)	3e (4-F)	5g (4-N(Me) ₂)	5i (4-OMe)
N1–N2	1.401(3)	1.413(2)	1.401(3)	1.409(3)	1.411(3)	1.410(3)
N1–C6	1.273(3)	1.283(2)	1.280(3)	1.280(3)	1.285(4)	1.285(3)
N2–C7	1.266(3)	1.267(2)	1.260(3)	1.265(3)	1.272(4)	1.258(4)
C1–C6	1.470(3)	1.466(2)	1.465(3)	1.463(3)	1.460(4)	1.465(4)
C7–C8	1.458(4)	1.463(2)	1.458(3)	1.456(3)	1.457(4)	1.452(4)
C6–N1–N2	114.2(2)	113.41(14)	114.62(18)	113.77(17)	114.4(2)	113.1(2)
C7–N2–N1	112.5(2)	111.33(14)	112.25(18)	111.73(18)	111.9(3)	112.2(3)
N1–C6–C1	117.3(2)	116.26(13)	116.26(19)	115.87(17)	116.0(3)	115.8(3)
N2–C7–C8	122.4(2)	122.10(15)	122.83(19)	121.72(19)	124.0(3)	123.1(3)
C6–N1–N2–C7	174.3(2)	177.70(14)	162.1(2)	177.40(18)	172.2(3)	179.0(3)
N2–N1–C6–C1	178.6(2)	178.33(13)	179.17(18)	178.75(16)	180.0(2)	177.3(2)
N1–N2–C7–C8	177.8(2)	179.07(13)	179.99(19)	177.50(17)	179.1(3)	177.0(3)
N3–N4					1.415(3)	1.418(4)
N3–C22					1.291(3)	1.287(4) ^a
N4–C23					1.277(3)	1.268(4) ^b
C22–C17					1.470(4)	1.465(5) ^c
C23–C24					1.443(4)	1.459(5) ^d
C22–N3–N4					113.2(3)	112.2(3) ^e
C24–N4–N3					111.1(3)	112.9(3) ^f
N3–C22–C17					115.7(3)	116.1(3) ^g
N4–C23–C24					122.7(3)	121.9(3) ^h
C22–N3–N4–C23					163.6(3)	160.1(3) ⁱ
N4–N3–C22–C17					–178.9(2)	–176.7(3) ^j
N3–N4–C23–C24					–175.5(3)	–176.8(3) ^k

^aN3–C21. ^bN4–C22. ^cC21–C16. ^dC22–C23. ^eC21–N3–N4. ^fC23–N4–N3. ^gN3–C21–C16. ^hN4–C22–C23. ⁱC21–N3–N4–C22. ^jN4–N3–C21–C16. ^kN3–N4–C22–C23.

Table 5. Dihedral Angles (deg) between the Planes of the Molecular Parts

	dihedral angle	
	cyclopentadienyl and plane ^a	aryl rings and plane ^a
3e (4-F)	10.3	4.8
3d (4-Cl)	12.7	11.8
3f (4-CH ₃)	4.2	3.7
3k (4-OCH ₃)	4.2	7.2
5i (4-OCH ₃)	6.6	4.9
5g (4-N(CH ₃) ₂)	6.4	8.4

^aPlane: the central C=N–N=C moiety.

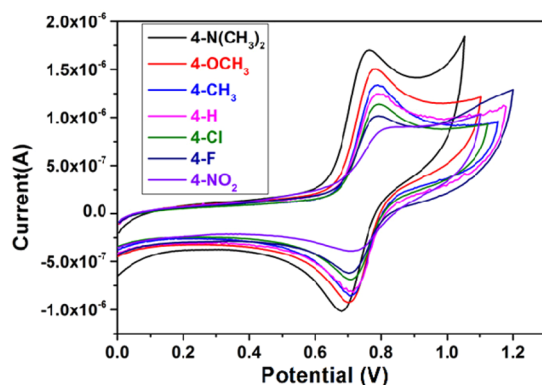


Figure 2. Cyclic voltammetry of selected monosubstituted ferrocenyl-based unsymmetrical azines in CH₃CN solution at 0.1 V s^{−1} scan rate.

containing electron-donating groups on the aryl moiety (ferrocenyl/4-OCH₃) had a larger, more significant contribution on the azine –C=N–N=C– unit, as determined by the

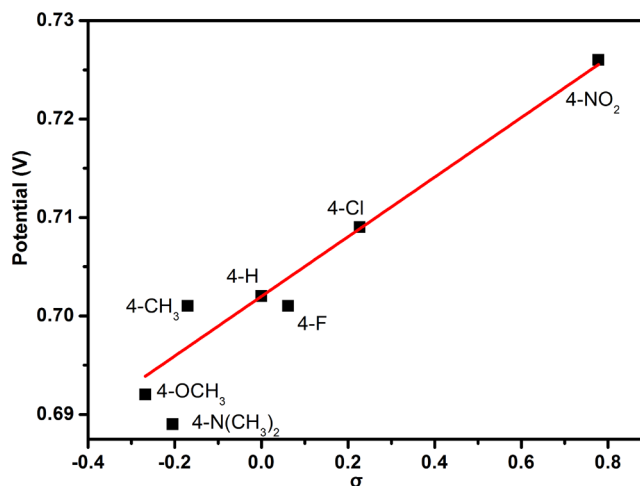


Figure 3. Hammett-type plot of σ versus E° measured in CH₃CN solution at 0.1 V s^{−1}. Hammett σ values: 4-F, 0.062; 4-NO₂, 0.778; 4-H, 0; 4-OCH₃, −0.268; 4-CH₃, −0.17; 4-Cl, 0.227; 4-N(CH₃)₂, −0.205.

calculations. This provided further support for the conclusions from the electrochemical and optical studies. In contrast with the aryl-substituted azine, the ferrocenyl-substituted azines have more extensive conjugation. The ferrocenyl-substituted azine (ferrocenyl/4-OCH₃) is expected to have complete conjugation.

CONCLUSIONS

In summary, we have designed and synthesized 1-substituted and 1,1'-disubstituted ferrocene-based unsymmetrical azines under metal-free conditions. The crystal structures of 3k, 5i,

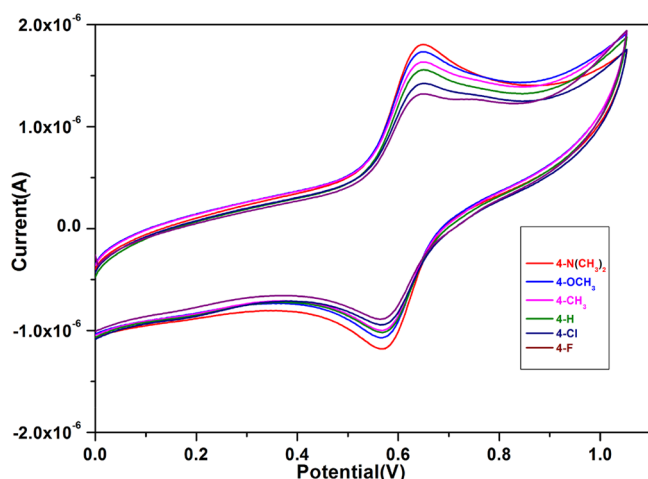


Figure 4. Cyclic voltammetry of selected 1,1'-disubstituted ferrocenyl-based unsymmetrical azines in CH_3CN solution at 0.1 V s^{-1} scan rate.

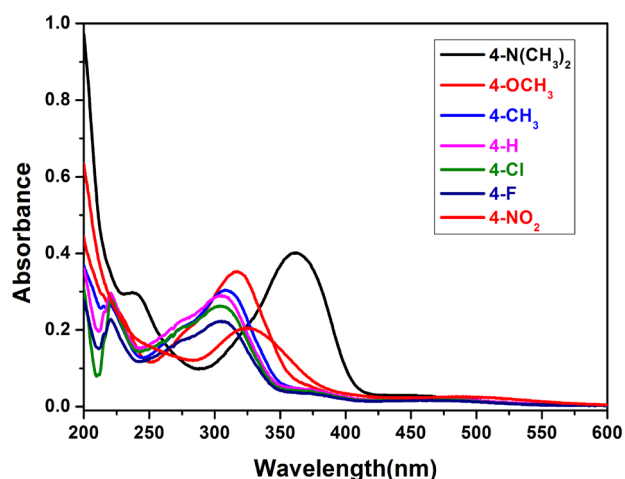


Figure 5. UV-vis spectra of selected monosubstituted ferrocenyl-based unsymmetrical azines in CH_3CN solution.

Table 6. UV-Vis Spectral Data for Selected Monosubstituted Ferrocenyl-Based Unsymmetrical Azines in CH_3CN Solution

substituent group	λ_{max} (nm)
3e (4-F)	300
3d (4-Cl)	302
3a (4-H)	306
3f (4-CH ₃)	311
3k (4-OCH ₃)	324
3i (4-N(CH ₃) ₂)	365
3h (4-NO ₂)	326

and **5g** revealed that conjugative interactions between the ferrocene phenyl rings with the entire azine fragment exist. The liquid-state study of ferrocenyl-based unsymmetrical azines provided support for extended conjugation, which suggested a larger substituent effect in this system. Calculations provided further support for the conclusions from the electrochemical and optical studies. Therefore, these results reflect a stronger conjugative interaction. The resulting 1-substituted azine **3m** and 1,1'-disubstituted ferrocene-based unsymmetrical azine **5k** derivatives have been shown to be excellent multichannel recognition receptors for Hg^{2+} and Cu^{2+} ions. Further

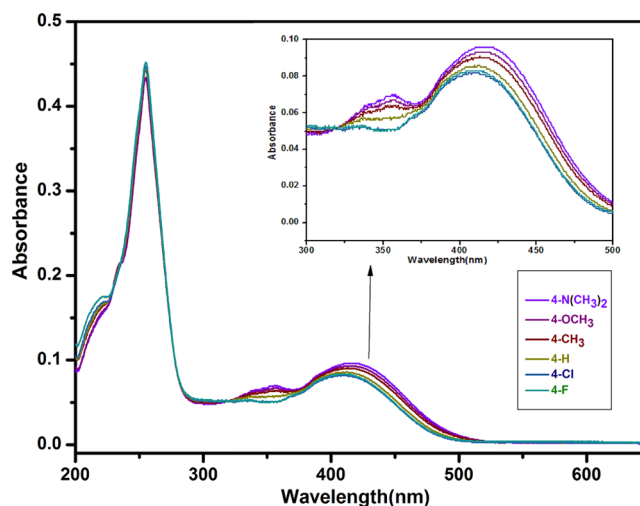


Figure 6. UV-vis spectra of selected 1,1'-disubstituted ferrocenyl-based unsymmetrical azines in CH_3CN solution.

experiments in the design of more efficient and selective ferrocene-based receptors are currently under way in our laboratory, and the results will be reported in due course.

EXPERIMENTAL SECTION

General Information. All reagents were used as received from commercial sources, unless specified otherwise, or prepared as described in the literature. All solvents were purified by following standard literature procedures. For chromatography, 200–300 mesh silica gel (Qingdao, China) was employed. All NMR experiments were carried out on a Bruker Avance 500 spectrometer using CDCl_3 as the solvent with tetramethylsilane as the internal standard. Chemical shift values (δ) are given in parts per million. Electrospray mass (ESI-MS) spectra were recorded on a Bruker QTOF mass instrument. Melting points were determined with a melting point apparatus and are uncorrected. The UV-vis absorption spectra were recorded with a UV-2700 instrument (Shimadzu) at room temperature. The CV and DPV measurements were carried out on a Metrohm Autolab B. V. instrument. An Ag/AgCl electrode was used as the reference electrode, a platinum wire was used as the counter electrode, and Pt was used as the working electrode. DFT calculations were performed using the B3LYP functional³¹ and 6-31G* basis set³² as implemented in Gaussian 09.³³

General Procedure for Metal-Free Reaction and Spectral Data of Products. Aldehyde **1a** (53.1 mg, 0.5 mmol), hydrazine **2a** (99.1 mg, 0.25 mmol), $t\text{-BuOLi}$ (22.0 mg, 0.275 mmol), and PPh_3 (131.2 mg, 0.5 mmol) were suspended in dioxane (5 mL) in a 25 mL Schlenk tube under nitrogen. The solution was stirred at 90°C for 16 h. Then the reaction mixture was cooled to ambient temperature, diluted with 20 mL of CH_2Cl_2 , and washed with brine (20 mL) and water (20 mL). The organic layers were combined and dried over MgSO_4 and filtered. The solvents were evaporated under reduced pressure, and the residue was purified by flash chromatography on silica gel.

1-Benzylidene-2-(1-ferrocenylethylidene)hydrazine (3a).⁹ 1-Benzylidene-2-(1-ferrocenylpropylidene)hydrazine (**3b**): red oil, 49.9 mg (58% yield); R_f (petroleum ether/ethyl acetate 10/1) = 0.53; ^1H NMR (500 MHz, CDCl_3) δ 8.42 (s, 1H), 7.88–7.78 (d, J = 8.5 Hz, 2H), 7.46–7.39 (m, 3H), 4.77 (m, 2H), 4.47–4.41 (m, 2H), 4.21 (s, 5H), 2.92 (q, J = 7.5 Hz, 2H), 1.23 (t, J = 7.5 Hz, 3H); ^{13}C NMR (126 MHz, CDCl_3) δ 172.9, 157.0, 135.3, 130.7, 128.9, 128.8, 128.2, 128.1, 81.6, 70.7, 69.6, 69.5, 67.9, 23.9, 13.3; HRMS (ESI-TOF) m/z [M]⁺ calcd for $\text{C}_{20}\text{H}_{20}\text{FeN}_2$ 344.0976, found 344.0971.

1-Benzylidene-2-(1-ferrocenylbutylidene)hydrazine (3c).⁹ 1-(4-Chlorobenzylidene)-2-(1-ferrocenylethylidene)hydrazine (**3d**): red solid, 63.8 mg (70% yield); mp 103 – 105°C ; R_f (petroleum ether/ethyl acetate 10/1) = 0.45; ^1H NMR (500 MHz, CDCl_3) δ 8.37

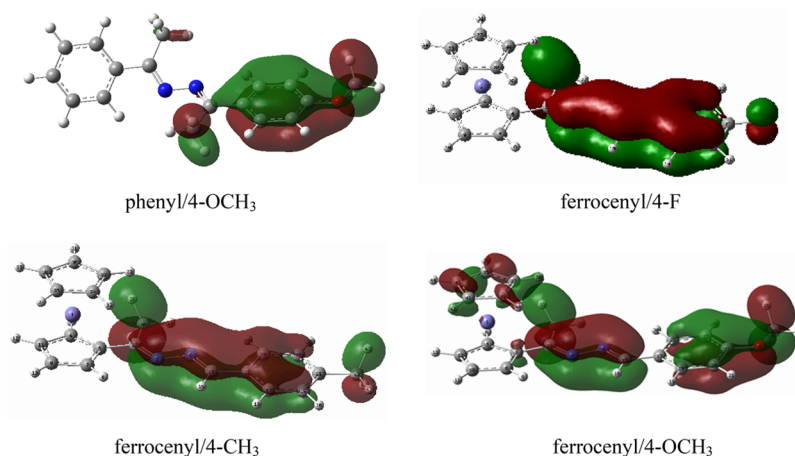


Figure 7. HOMOs of selected phenyl and ferrocenyl unsymmetrical azines, respectively, determined by B3LYP/6-31G* calculations.

(s, 1H), 7.75 (d, J = 8.4 Hz, 2H), 7.39 (d, J = 8.4 Hz, 2H), 4.76 (m, 2H), 4.42 (m, 2H), 4.20 (s, 5H), 2.42 (s, 3H). ^{13}C NMR (126 MHz, CDCl_3) δ 168.2, 156.0, 136.4, 133.6, 129.4, 129.0, 82.5, 70.7, 69.5, 68.0, 16.2; HRMS (ESI-TOF) m/z $[\text{M}]^+$ calcd for $\text{C}_{19}\text{H}_{17}\text{ClFeN}_2$ 364.0430, found 364.0426.

1-(4-Fluorobenzylidene)-2-(1-ferrocenylethylidene)-hydrazine (3e): red solid, 60.0 mg (69% yield); mp 108–110 °C; R_f (petroleum ether/ethyl acetate 10/1) = 0.44; ^1H NMR (500 MHz, CDCl_3) δ 8.38 (s, 1H), 7.81 (d, J = 8.4 Hz, 2H), 7.11 (m, 2H), 4.76 (m, 2H), 4.42 (m, 2H), 4.20 (s, 5H), 2.42 (s, 3H); ^{13}C NMR (126 MHz, CDCl_3) δ 167.9, 165.2, 163.2, 156.0, 131.4, 130.1, 130.0, 116.0, 115.8, 82.6, 70.7, 69.5, 67.9, 16.1; HRMS (ESI-TOF) m/z $[\text{M}]^+$ calcd for $\text{C}_{19}\text{H}_{17}\text{FeN}_2$ 348.0725, found 348.0722.

2-(1-Ferrocenylethylidene)-1-(4-methylbenzylidene)-hydrazine (3f): red solid, 51.7 mg (60% yield); mp 110–112 °C; R_f (petroleum ether/ethyl acetate 10/1) = 0.46; ^1H NMR (500 MHz, CDCl_3) δ 8.38 (s, 1H), 7.72 (d, J = 8.0 Hz, 2H), 7.23 (d, J = 8.0 Hz, 2H), 4.82–4.69 (m, 2H), 4.47–4.33 (m, 2H), 4.19 (s, 5H), 2.42 (s, 3H), 2.39 (s, 3H); ^{13}C NMR (126 MHz, CDCl_3) δ 167.2, 157.3, 140.8, 132.4, 129.5, 128.2, 82.8, 70.5, 69.5, 67.9, 21.7, 16.1; HRMS (ESI-TOF) m/z $[\text{M}]^+$ calcd for $\text{C}_{20}\text{H}_{20}\text{FeN}_2$ 344.0976, found 344.0973.

2-(1-Ferrocenylethylidene)-1-(2-nitrobenzylidene)hydrazine (3g): aubergine oil, 37.5 mg (40% yield); R_f (petroleum ether/ethyl acetate 10/1) = 0.28; ^1H NMR (500 MHz, CDCl_3) δ 8.80 (s, 1H), 8.24 (d, J = 8.0 Hz, 1H), 8.00 (d, J = 7.5 Hz, 1H), 7.67 (m, 1H), 7.60–7.53 (m, 1H), 4.78 (m, 2H), 4.45 (m, 2H), 4.21 (s, 5H), 2.39 (s, 3H); ^{13}C NMR (126 MHz, CDCl_3) δ 168.7, 152.1, 148.9, 137.3, 133.1, 130.5, 129.4, 124.6, 82.1, 70.9, 69.6, 68.2, 16.3; HRMS (ESI-TOF) m/z $[\text{M}]^+$ calcd for $\text{C}_{19}\text{H}_{17}\text{FeN}_3\text{O}_2$ 375.0670, found 375.0664.

2-(1-Ferrocenylethylidene)-1-(4-nitrobenzylidene)hydrazine (3h): ^{9,28} *N,N*-Dimethyl-4-(((1-ferrocenylethylidene)-hydrazono)methyl)aniline (3i): orange solid, 50.4 mg (54% yield); mp 64–66 °C; R_f (petroleum ether/ethyl acetate 10/1) = 0.25; ^1H NMR (500 MHz, CDCl_3) δ 8.35 (s, 1H), 7.71 (d, J = 8.8 Hz, 2H), 6.72 (d, J = 8.8 Hz, 2H), 4.75 (m, 2H), 4.49–4.31 (m, 2H), 4.20 (s, 5H), 3.03 (s, 6H), 2.44 (s, 3H); ^{13}C NMR (126 MHz, CDCl_3) δ 165.8, 157.9, 152.1, 129.8, 123.0, 111.8, 83.4, 70.3, 69.4, 67.7, 40.3, 16.0; HRMS (ESI-TOF) m/z $[\text{M}]^+$ calcd for $\text{C}_{21}\text{H}_{23}\text{FeN}_3$ 373.1241, found 373.1238.

2-(1-Ferrocenylethylidene)-1-(2-methoxybenzylidene)-hydrazine (3j): ⁹ **2-(1-Ferrocenylethylidene)-1-(4-methoxybenzylidene)hydrazine (3k):** ⁹ **1-(1-Ferrocenylethylidene)-2-(thiophen-2-ylmethylene)hydrazine (3l):** red oil, 47.1 mg (56% yield); R_f (petroleum ether/ethyl acetate 10/1) = 0.46; ^1H NMR (500 MHz, CDCl_3) δ 8.56 (s, 1H), 7.42 (d, J = 5.0 Hz, 1H), 7.36 (d, J = 3.4 Hz, 1H), 7.14–7.06 (m, 1H), 4.75 (m, 2H), 4.42 (m, 2H), 4.19 (s, 5H), 2.41 (s, 3H); ^{13}C NMR (126 MHz, CDCl_3) δ 168.1, 151.3, 140.4, 131.0, 129.0, 127.7, 82.6, 70.7, 69.5, 67.9, 16.1;

HRMS (ESI-TOF) m/z $[\text{M}]^+$ calcd for $\text{C}_{17}\text{H}_{16}\text{FeN}_2\text{S}$ 336.0384, found 336.0371.

1-(Anthracen-9-ylmethylene)-2-(1-ferrocenylethylidene)-hydrazine (3m): ^{9,26} **1,1'-Bis(1-(benzylidenehydrazono)ethyl)-ferrocene (5a):** ²⁷ **1,1'-Bis(1-(benzylidenehydrazono)propyl)-ferrocene (5b):** red oil, 41.4 mg (33% yield); R_f (petroleum ether/ethyl acetate 5/1) = 0.40; ^1H NMR (500 MHz, CDCl_3) δ 8.39 (s, 2H), 7.82–7.77 (d, J = 8.6 Hz, 4H), 7.45–7.39 (m, 6H), 4.80 (m, 4H), 4.49–4.42 (m, 4H), 2.88 (q, J = 7.6 Hz, 4H), 1.18 (t, J = 7.6 Hz, 6H); ^{13}C NMR (126 MHz, CDCl_3) δ 172.0, 157.2, 135.2, 130.4, 128.9, 128.7, 128.3, 128.2, 82.9, 13.2; HRMS (ESI-TOF) m/z $[\text{M} + \text{H}]^+$ calcd for $\text{C}_{30}\text{H}_{30}\text{FeN}_4$ 503.1898, found 503.1893.

1,1'-Bis(1-(benzylidenehydrazono)butyl)ferrocene (5c): red oil, 39.8 mg (30% yield); R_f (petroleum ether/ethyl acetate 5/1) = 0.41; ^1H NMR (500 MHz, CDCl_3) δ 8.40 (s, 2H), 7.79 (d, J = 8.6 Hz, 4H), 7.44–7.38 (m, 6H), 4.89–4.73 (m, 4H), 4.52–4.42 (m, 4H), 2.94–2.79 (t, J = 7.5 Hz, 4H), 1.64 (m, 4H), 0.97 (t, J = 7.4 Hz, 6H); ^{13}C NMR (126 MHz, CDCl_3) δ 171.0, 157.3, 135.3, 130.4, 128.7, 128.3, 83.3, 72.0, 69.2, 32.5, 22.2, 14.8; HRMS (ESI-TOF) m/z $[\text{M} + \text{H}]^+$ calcd for $\text{C}_{32}\text{H}_{34}\text{FeN}_4$ 531.2211, found 531.2211.

1,1'-Bis(1-((4-chlorobenzylidene)hydrazono)ethyl)ferrocene (5d): red oil, 63.8 mg (47% yield); R_f (petroleum ether/ethyl acetate 5/1) = 0.31; ^1H NMR (500 MHz, CDCl_3) δ 8.31 (s, 2H), 7.65 (d, J = 8.4 Hz, 4H), 7.32 (d, J = 8.4 Hz, 4H), 4.90–4.72 (m, 4H), 4.52–4.40 (m, 4H), 2.37 (s, 6H); ^{13}C NMR (126 MHz, CDCl_3) δ 167.4, 156.2, 136.4, 133.5, 129.4, 129.0, 83.8, 71.8, 69.2, 16.1; HRMS (ESI-TOF) m/z $[\text{M} + \text{H}]^+$ calcd for $\text{C}_{28}\text{H}_{24}\text{Cl}_2\text{FeN}_4$ 543.0805, found 543.0804.

1,1'-Bis(1-((4-fluorobenzylidene)hydrazono)ethyl)ferrocene (5e): red oil, 57.4 mg (45% yield); R_f (petroleum ether/ethyl acetate 5/1) = 0.30; ^1H NMR (500 MHz, CDCl_3) δ 8.34 (s, 2H), 7.73 (d, J = 8.6 Hz, 4H), 7.05 (m, 4H), 4.90–4.72 (m, 4H), 4.50–4.39 (m, 4H), 2.38 (s, 6H); ^{13}C NMR (126 MHz, CDCl_3) δ 167.1, 165.2, 163.2, 156.2, 131.3, 131.3, 130.1, 130.1, 115.9, 115.8, 83.9, 71.8, 69.1, 16.1; HRMS (ESI-TOF) m/z $[\text{M} + \text{H}]^+$ calcd for $\text{C}_{28}\text{H}_{24}\text{F}_2\text{FeN}_4$ 511.1396, found 511.1392.

1,1'-Bis(1-((4-methylbenzylidene)hydrazono)ethyl)-ferrocene (5f): red solid, 50.2 mg (40% yield); mp 134–136 °C; R_f (petroleum ether/ethyl acetate 5/1) = 0.41; ^1H NMR (500 MHz, CDCl_3) δ 8.35 (s, 2H), 7.66 (d, J = 7.8 Hz, 4H), 7.18 (d, J = 7.8 Hz, 4H), 4.78 (m, 4H), 4.43 (m, 4H), 2.41 (s, 6H), 2.38 (s, 6H); ^{13}C NMR (126 MHz, CDCl_3) δ 166.4, 157.5, 140.8, 132.3, 129.4, 128.2, 84.0, 71.7, 69.0, 21.6, 16.1; HRMS (ESI-TOF) m/z $[\text{M} + \text{H}]^+$ calcd for $\text{C}_{30}\text{H}_{30}\text{FeN}_4$ 503.1898, found 503.1893.

1,1'-Bis(1-((4-dimethylaminobenzylidene)hydrazono)ethyl)-ferrocene (5g): orange solid, 42.0 mg (30% yield); mp 171–173 °C; R_f (petroleum ether/ethyl acetate 2.5/1) = 0.34; ^1H NMR (500 MHz, CDCl_3) δ 8.33 (s, 2H), 7.68 (d, J = 8.8 Hz, 4H), 6.69 (d, J = 8.8 Hz, 4H), 5.07–4.57 (m, 4H), 4.52–4.14 (m, 4H), 3.03 (s, 12H), 2.41 (s, 6H); ^{13}C NMR (126 MHz, CDCl_3) δ 165.1, 158.0, 152.0, 129.8,

123.1, 111.8, 84.5, 71.6, 68.8, 40.3, 16.0; HRMS (ESI-TOF) m/z $[M + H]^+$ calcd for $C_{32}H_{36}FeN_6$ 561.2429, found 561.2426.

1,1'-Bis(1-((2-methoxybenzylidene)hydrazono)ethyl)-ferrocene (5h): red solid, 37.4 mg (28% yield); mp 155–157 °C; R_f (petroleum ether/ethyl acetate 5/1) = 0.26; 1H NMR (500 MHz, $CDCl_3$) δ 8.80 (s, 2H), 8.07 (d, J = 8.7 Hz, 2H), 7.43–7.34 (d, J = 8.7 Hz, 2H), 6.99–6.88 (m, 4H), 4.85–4.75 (m, 4H), 4.48–4.38 (m, 4H), 3.85 (s, 6H), 2.39 (s, 6H); ^{13}C NMR (126 MHz, $CDCl_3$) δ 166.1, 158.9, 153.3, 131.8, 127.2, 123.7, 120.8, 111.2, 84.2, 71.7, 68.9, 55.6, 16.1; HRMS (ESI-TOF) m/z $[M + H]^+$ calcd for $C_{30}H_{30}FeN_4O_2$ 535.1796, found 535.1791.

1,1'-Bis(1-((4-methoxybenzylidene)hydrazono)ethyl)-ferrocene (5i).²⁹ **1,1'-Bis(1-((thiophen-2-ylmethylene)hydrazono)ethyl)ferrocene (5j):** red oil, 41.3 mg (34% yield); R_f (petroleum ether/ethyl acetate 5/1) = 0.32; 1H NMR (500 MHz, $CDCl_3$) δ 8.53 (s, 2H), 7.40 (d, J = 5.0 Hz, 2H), 7.30 (d, J = 3.5 Hz, 2H), 7.06 (m, 2H), 4.87–4.67 (m, 4H), 4.47–4.41 (m, 4H), 2.38 (s, 6H); ^{13}C NMR (126 MHz, $CDCl_3$) δ 167.2, 151.6, 140.4, 131.1, 129.0, 127.7, 83.9, 71.9, 69.2, 16.1; HRMS (ESI-TOF) m/z $[M + H]^+$ calcd for $C_{24}H_{22}FeN_4S_2$ 487.0713, found 487.0706.

■ ASSOCIATED CONTENT

Supporting Information

1,1'-Bis(1-((anthracen-9-ylmethylene)hydrazono)ethyl)-ferrocene (5k).⁹The Supporting Information is available free of charge on the ACS Publications website at DOI: 10.1021/acs.organomet.7b00366.

1H NMR and ^{13}C NMR spectra for the products, crystal and structure refinement data for complexes **3d** (4-Cl), **3e** (4-F), **3f** (4-Me), **3k** (4-OMe), **5g** (4-N(Me)₂), and **5i** (4-OMe), and details of DFT computations (PDF)

Accession Codes

CCDC 1548571–1548576 contain the supplementary crystallographic data for this paper. These data can be obtained free of charge via www.ccdc.cam.ac.uk/data_request/cif, or by emailing data_request@ccdc.cam.ac.uk, or by contacting The Cambridge Crystallographic Data Centre, 12 Union Road, Cambridge CB2 1EZ, UK; fax: +44 1223 336033.

■ AUTHOR INFORMATION

Corresponding Author

*H.Z.: tel, +86-471-4994406; fax, +86-471-4994406; e-mail, haozhang@imu.edu.cn and zh_hjf@hotmail.com.

ORCID

Yi Luo: 0000-0001-6390-8639

Hao Zhang: 0000-0003-2249-3179

Notes

The authors declare no competing financial interest.

■ ACKNOWLEDGMENTS

This work was financially supported by the National Science Foundation of China (No. 21364005) and Grassland Talent Innovative Teams of Inner Mongolia Autonomous Region, and the project was supported by the Open Research Fund of State Key Laboratory of Polymer Physics and Chemistry, Changchun Institute of Applied Chemistry, Chinese Academy of Sciences.

■ REFERENCES

- (1) Khodair, A. I.; Bertrand, P. *Tetrahedron* **1998**, *54*, 4859–4872.
- (2) Astheimer, H.; Walz, L.; Haase, W.; Loub, J.; Müller, H. J.; Gallardo, M. *Mol. Cryst. Liq. Cryst.* **1985**, *131*, 343–351.
- (3) Singh, B.; Pandey, A. *Liq. Cryst.* **2009**, *37*, 57–67.

- (4) Singh, B.; Pandey, A. *Mol. Cryst. Liq. Cryst.* **2010**, *517*, 148–158.
- (5) Hauer, C. R.; King, G. S.; McCool, E. L.; Euler, W. B.; Ferrara, J. D.; Youngs, W. J. *J. Am. Chem. Soc.* **1987**, *109*, 5760–5765.
- (6) Dudis, D. S.; Yeates, A. T.; Kost, D.; Smith, D. A.; Medrano, J. J. *Am. Chem. Soc.* **1993**, *115*, 8770–8774.
- (7) Granifo, J.; Vargas, M. E.; Dodsworth, E. S.; Farrar, D. H.; Fielder, S. S.; Lever, A. B. P. *J. Chem. Soc., Dalton Trans.* **1996**, *23*, 4369–4378.
- (8) Caballero, A.; Martínez, R.; Lloveras, V.; Ratera, I.; Vidal-Gancedo, J.; Wurst, K.; Tárraga, A.; Molina, P.; Veciana, J. *J. Am. Chem. Soc.* **2005**, *127*, 15666–15667.
- (9) Liu, Y. F.; Teng, Q.; Hu, J. F.; Sun, R. F.; Zhang, H. *Sens. Actuators, B* **2016**, *234*, 680–690.
- (10) Chen, G. S.; Anthamatten, M.; Barnes, C. L.; Glaser, R. J. *Org. Chem.* **1994**, *59*, 4336–4340.
- (11) Sauro, V. A.; Workentin, M. S. *J. Org. Chem.* **2001**, *66*, 831–838.
- (12) Safari, J.; Gandomi-Ravandi, S. *RSC Adv.* **2014**, *4*, 46224–46249.
- (13) Barluenga, J.; Moriel, P.; Valdés, C.; Aznar, F. *Angew. Chem., Int. Ed.* **2007**, *46*, 5587–5590.
- (14) Feng, X. W.; Wang, J.; Zhang, J.; Yang, J.; Wang, N.; Yu, X. Q. *Org. Lett.* **2010**, *12*, 4408–4411.
- (15) Zhou, L.; Ye, F.; Ma, J.; Zhang, Y.; Wang, J. *Angew. Chem.* **2011**, *123*, 3572–3576.
- (16) Zhou, L.; Shi, Y.; Xiao, Q.; Liu, Y.; Ye, F.; Zhang, Y.; Wang, J. *Org. Lett.* **2011**, *13*, 968–971.
- (17) Ye, F.; Ma, X.; Xiao, Q.; Li, H.; Zhang, Y.; Wang, J. *J. Am. Chem. Soc.* **2012**, *134*, 5742–5745.
- (18) Zhao, X.; Wu, G.; Zhang, Y.; Wang, J. *J. Am. Chem. Soc.* **2011**, *133*, 3296–3299.
- (19) Yao, T.; Hirano, K.; Satoh, T.; Miura, M. *Angew. Chem., Int. Ed.* **2012**, *51*, 775–779.
- (20) Barluenga, J.; Tomás-Gamasa, M.; Aznar, F.; Valdés, C. *Nat. Chem.* **2009**, *1*, 494–499.
- (21) Zhao, X.; Jing, J.; Lu, K.; Zhang, Y.; Wang, J. *Chem. Commun.* **2010**, *46*, 1724–1726.
- (22) Xiao, Q.; Ma, J.; Yang, Y.; Zhang, Y.; Wang, J. *Org. Lett.* **2009**, *11*, 4732–4735.
- (23) Sha, Q.; Ling, Y.; Wang, W.; Wei, Y. *Adv. Synth. Catal.* **2013**, *355*, 2145–2150.
- (24) Sha, Q.; Wei, Y. *ChemCatChem* **2014**, *6*, 131–134.
- (25) Teng, Q.; Hu, J. F.; Ling, L.; Sun, R. F.; Dong, J. Y.; Chen, S. F.; Zhang, H. *Org. Biomol. Chem.* **2014**, *12*, 7721–7727.
- (26) Houlton, A.; Jasim, N.; Roberts, R. M. G.; Silver, J.; Cunningham, D.; McArdle, P.; Higgins, T. *J. Chem. Soc., Dalton Trans.* **1992**, 2235–2241.
- (27) Sauro, V. A.; Workentin, M. S. *Can. J. Chem.* **2002**, *80*, 250–262.
- (28) López, C.; Bosque, R.; Arias, J.; Evangelio, E.; Solans, X.; Font-Bardía, M. *J. Organomet. Chem.* **2003**, *672*, 34–42.
- (29) Qiao, C. J.; Li, J.; Xu, Y.; Guo, S. Y.; Qi, X.; Fan, Y. T. *Appl. Organomet. Chem.* **2009**, *23*, 421–424.
- (30) Levine, I. N. *J. Chem. Phys.* **1963**, *38*, 2326–2328.
- (31) Becke, A. D. A New Mixing of Hartree-Fock and Local Density-Functional Theories. *J. Chem. Phys.* **1993**, *98*, 1372–1377.
- (32) Francl, M. M.; Pietro, W. J.; Hehre, W. J.; Binkley, J. S.; Gordon, M. S.; Defrees, D. J.; Pople, J. A. Self-Consistent Molecular Orbital Methods. XXIII. A Polarization-Type Basis Set for Second-Row Elements. *J. Chem. Phys.* **1982**, *77*, 3654–3665.
- (33) Frisch, M. J.; Schlegel, H. B.; Scuseria, G. E.; Robb, M. A.; Cheeseman, J. R.; Scalmani, G.; Barone, V.; Mennucci, B.; Petersson, G. A.; Nakatsuji, H.; Caricato, M.; Li, X.; Hratchian, H. P.; Izmaylov, A. F.; Bloino, J.; Zheng, G.; Sonnenberg, J. L.; Hada, M.; Ehara, M.; Toyota, K.; Fukuda, R.; Hasegawa, J.; Ishida, M.; Nakajima, T.; Honda, Y.; Kitao, O.; Nakai, H.; Vreven, T.; Montgomery, J. A., Jr.; Peralta, F.; Ogliaro, M.; Bearpark, J. J.; Heyd, E.; Brothers, K. N.; Kudin, V. N.; Staroverov, R.; Kobayashi, J.; Normand, K.; Raghavachari, A.; Rendell, J. C.; Burant, S. S.; Iyengar, J.; Tomasi, M.; Cossi, N.; Rega, J. M.; Millam, M.; Klene, J. E.; Knox, J. B.; Cross, V.; Bakken, C.; Adamo, J.; Jaramillo, R.; Gomperts, R. E.; Stratmann, O.; Yazyev, A. J.; Austin, R.

Cammi, C.; Pomelli, J. W.; Ochterski, R. L.; Martin, K.; Morokuma, V. G.; Zakrzewski, G. A.; Voth, P.; Salvador, J. J.; Dannenberg, S.; Dapprich, A. D.; Daniels, O.; Farkas, J. B.; Foresman, J. V.; Ortiz, J.; Cioslowski, J.; Fox, D. J. *GAUSSIAN 09, Revision E.01*; Gaussian, Inc., Wallingford, CT, 2009.